GEOPHYSICS, VOL. 54, NO. 12 (DECEMBER 1989); P. 1528–1534, 10 FIGS., 1 TABLE.

Mapping a bedrock surface under dry alluvium with shallow seismic reflections

Richard D. Miller*, Don W. Steeples*, and Michael Brannan‡

ABSTRACT

Shallow seismic-reflection techniques were used to image the bedrock-alluvial interface, near a chemical evaporation pond in the Texas Panhandle, allowing optimum placement of water-quality monitor wells. The seismic data showed bedrock valleys as shallow as 4 m and accurate to within 1 m horizontally and vertically. The normal-moveout velocity within the near-surface alluvium varies from 225 m/s to 400 m/s. All monitor-well borings near the evaporation pond penetrated unsaturated alluvial material. On most of the data, the wavelet reflected from the bedrock-alluvium interface has a dominant frequency of around 170 Hz. Low-cut filtering at 24 dB/octave below 220 Hz prior to analog-to-digital conversion enhanced the amplitude of the desired bedrock reflection relative to the amplitude of the unwanted ground roll. The final bedrock contour map derived from drilling and seismic-reflection data possesses improved resolution and shows a bedrock valley not interpretable from drill data alone.

INTRODUCTION

Detailed knowledge of the bedrock surface is often crucial in planning well locations for groundwater-quality monitoring. Changes in groundwater quality often first appear in monitor wells located in topographic lows in the bedrock surface. Data possessing the necessary detail for conclusive bedrock surface mapping have generally come from extensive drilling programs which are time-consuming, expensive, and environmentally undesirable. High-resolution seismic-reflection profiling has been used to image surfaces as shallow as 3 m and resolve beds as thin as 1 m in a variety of near-surface geologic settings (Schepers, 1975; Doornenbal and Helbig, 1983; Birkelo et al., 1987; Myers et al., 1987; Branham and Steeples, 1988). Seismic reflection profiling has the potential to produce the necessary details of a shallow (4 m deep) bedrock surface to pinpoint optimum locations for monitor wells.

The bedrock-overburden contact has been mapped successfully using reflection seismology at depths greater than 20 m (Hunter et al., 1984). Using conventional shallow-reflection techniques, bedrock reflectors shallower than 20 m are difficult to separate from other energy arriving in the early portions of the seismograms (Steeples and Miller, 1986). The amplitudes of these shallow reflected waves at commonly recorded frequencies are smaller than the amplitudes of unwanted waves, particularly ground roll, refractions, and air-coupled waves. Detection of shallow reflecting events requires closely spaced source-receiver geometries, severe analog low-cut filtering, a suitable high-frequency seismic source, and a seismograph with quiet amplifiers and analog/digital (A/D) conversion into a large digital word (Knapp and Steeples, 1986). These criteria allow a minimum of unwanted energy to be recorded, which, in turn, allows identification of subtle shallow reflectors previously obscured using more common seismic-reflection procedures.

Typical energy sources for shallow engineering studies include sledge hammers (Hunter et al., 1981; Meidav, 1969), weight drops (Doornenbal and Helbig, 1983), and small explosive charges (Pakiser and Warrick, 1956). Under ideal conditions (water table within 1 m of ground surface, solid geophone and source ground coupling, etc.), at a depth of 100 m, the dominant frequency generated by any shallow seismic source could exceed 100 Hz (Miller et al., 1986). In areas where surface and very near-subsurface conditions are not conducive to the propagation of seismic energy, certain sources generate comparatively higher frequency and amplitude seismic energy than others (Pullan and MacAuley, 1987). Previous experience has shown surface projectile sources to be a cost-effective high-frequency source in areas with a deep water table and rough, rocky terrain (Miller and Steeples, 1986; Treadway et al., 1988).

Manuscript received by the Editor November 14, 1988; revised manuscript received June 19, 1989.
*Kansas Geological Survey, 1930 Constant Avenue, Campus West, University of Kansas, Lawrence, KS 66046-2598.
‡Phillips Petroleum Company, 149 Phillips Bldg. Annex, Bartlesville, OK 74004.

The objective of the reflection-profiling project discussed here was to determine the bedrock topography within 1 m horizontal and 0.5 m vertical resolution. Such high-resolution data would allow accurate placement of a minimum number of monitor wells into bedrock valleys.

HORIZONTAL AND VERTICAL RESOLUTION

Vertical and horizontal resolution are improved by increasing the dominant frequency and broadening the frequency spectrum of recorded reflection energy (Widess, 1973; Knapp and Steeples, 1986). This increase in the frequency of recorded energy can often be obtained by use of severe low-cut filtering, proper field equipment for the conditions encountered, and careful field procedures. Severe low-cut filtering effectively attenuates the lower frequency information (ground roll), which allows balancing of the spectrum toward higher frequencies. Also, by attenuating much of the high-amplitude, low-frequency information, analog gain of the seismic amplifiers can often be increased in the field to improve the signal-to-noise ratio.

The resolving potential of seismic-reflection data depends on dominant frequency (wavelength), surface-station spacing, timing accuracy, and accuracy of calculated average velocities. In our study, the receiver and shot locations were spaced at 1.2 m intervals, giving 0.6 m horizontal subsurface-interval coverage on the 12-fold common-depth-point (CDP) stacked data. Subsurface spacing of 0.6 m, reflector depths around 8 m, and dominant reflection frequencies around 170 Hz allowed 3–4 sample points within the first Fresnel zone of the bedrock reflector. With an average P-wave velocity of the dry alluvium measured at 300 m/s and dominant reflection frequencies around 170 Hz, the minimum bed resolution is about 0.2 m (using the 1/8 wavelength criterion of Widess, 1973). The average velocity from the surface to the reflecting interface and the origin time of the reflected event must be known within 25 m/s and ±0.5 ms, respectively, to obtain the necessary depth resolution (these values assume a 300 m/s average velocity and a depth of 6 m, both of which are quite representative of the actual data set). This degree of accuracy would result in a depth uncertainty of 0.65 m.

GEOLOGIC SETTING AND FIELD PROCEDURES

Drill data from around the evaporation pond in Hutchinson County, Texas, prior to the seismic survey showed a 3 to 15 m thick layer of dry alluvium overlying a Permian-aged red-bed sequence composed of limestones, shales, and dolomites. The variations in bedrock elevation as evidenced on the drill data (Figure 1) are caused primarily by an erosional surface of the Permian-aged red beds beneath the alluvium. The ground-surface topography is generally a subdued version of the major bedrock topography.

The seismic survey included three 12-fold CDP lines following the perimeter of the evaporation pond (Figure 2). The preliminary bedrock contour map, compiled from drill data only, shows the primary bedrock low on the north end of the pond (Figure 1). With maximum control needed on the north end of the pond, two lines were shot north of the pond in conjunction with one line east and one line west of the pond. The west line is a continuation of the southernmost line on the north end of the pond. The two parallel northern lines are separated by about 50 m.

The data were collected using a modified 30-06 hunting rifle and single undamped 100 Hz Mark Products geophones. The rifle was modified with a blast-containment device that reduced the amplitude of the air-coupled wave as well as contained any stray bullet or rock fragments. The source was centered between two sets of 12 live geophones with a source-to-closest-receiver distance of 3.7 m. The single 100 Hz geophones attenuate energy below 100 Hz and maintain a flat response to energy up to 1000 Hz. High-resolution compressional-wave surveys have generally had the best success with high natural-frequency geophones (Steeples and Knapp, 1982; Hunter et al., 1984; Myers et al.,

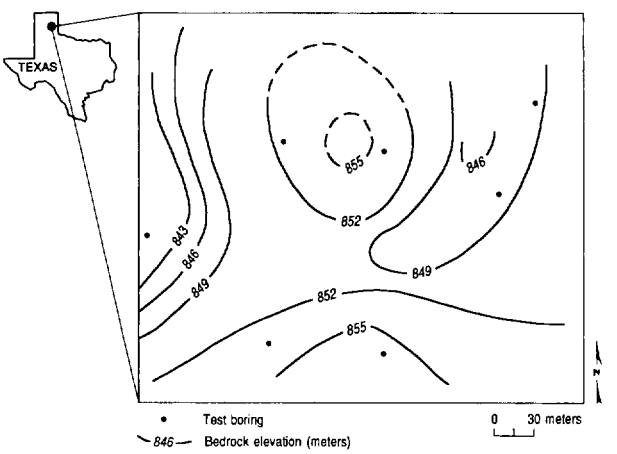

FIG. 1. Topography of the bedrock surface as defined by drill data.

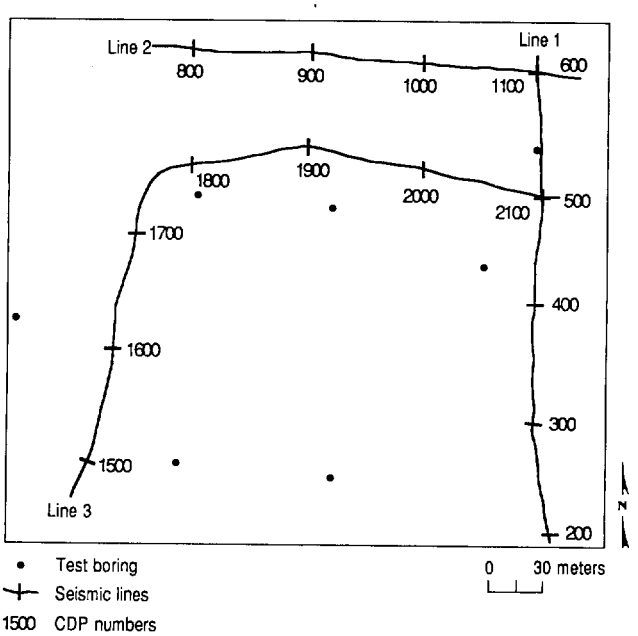

FIG. 2. Map view showing locations of the seismic lines, CDP numbers, and boreholes. The evaporation pond is located totally within the area defined by seismic lines 1 and 3 on the east, west, and north, and an imaginary line on the south between CDPs 1525 and 275.

1987). The close attention given to source-and-receiver ground coupling, which included consistent firing procedures, consistent geophone plants (securely and deeply planted), and careful manicuring of the ground surface prior to planting a geophone or firing a shot, improved frequency response and reduced unwanted noise.

An Input/Output DHR 2400 seismograph was used for recording the data on half-inch magnetic tape in modified SEG-Y format. The record length was 125 ms with a sample interval of 0.25 ms. Analog-to-digital (A/D) conversion resulted in a word length of 11 bits plus sign. The amplifiers have a factory noise specification of 120 nV rms, providing a fixed-gain dynamic range of 72 dB. Analog low-cut filters with 24 dB/octave rolloff and a −3 dB point at 220 Hz were used to maximize resolution and reduce the effects of ground roll. The reduction in unwanted noise as a result of the selected low-cut filters was essential to the quality and success of this survey.

DATA PROCESSING

Data were processed on a 32-bit Data General computer at the Kansas Geological Survey. The software used was a proprietary set of algorithms that has been in standard use on TIMAP seismic systems marketed by Texas Instruments. The processing flow is very similar to that used on seismic data for petroleum exploration (Table 1). The main distinctions were the emphasis and detail placed on near-surface velocity analysis and the extra care exercised in muting refracted arrivals.

Line 3 includes data collected around the northwest corner of the evaporation pond. This gentle bend in the line was compensated by applying the Pythogorean theorem by hand during the assignment of source and receiver geometries. Accurate velocity analysis was possible around the bend in the line as a result of this off-line compensation. The smearing effect resulting from the bend affected horizontal accuracy of individual CDPs location by less than 2 m. As a result of application of the Pythagorean theorem before normal-moveout (NMO) correction, vertical accuracy was compromised by less than 0.3 m.

The dry alluvium that overlies the bedrock showed extreme lateral variations in stacking velocity over very short horizontal distances. In certain areas, alluvial *P*-wave velocities fluctuated by 150 m/s (40%) in less than 50 m on the ground surface. With velocity changes this large, a detailed velocity function was required to optimize the NMO corrections producing sharp, clean reflecting events on the stacked sections. The suite of trial velocities applied to each CDP during velocity analysis included 25 different velocities incremented by 8 m/s between about 220 m/s and 420 m/s. Slight variation in the NMO velocity in this area can significantly affect the frequency, character, and apparent two-way traveltime of the resulting stacked wavelet (Figure 3).

The coherency of the stacked data was improved by a surface-consistent statics routine with a 1 ms (equivalent to about 1/6 of a wavelength) maximum allowable static shift. The statics operation enhanced the subtleties previously suspected on preliminary stacked sections. No processing procedure after the detailed velocity analysis altered the general interpretation of the data.

Table 1. Seismic data-processing flow chart.

(1)	Bad trace edit
(2)	Elevation statics
(3)	First-arrival mute
(4)	Spectral analysis
(5)	2nd zero crossing autopredictive deconvolution
(6)	Common-depth-point (CDP) sort
(7)	Velocity analysis
(8)	Surface-consistent statics
(9)	Band-pass filter
(10)	Automatic gain control (AGC) scale
(11)	Common-depth-point (CDP) stack

RESULTS

The bedrock reflector is the largest-amplitude and highest-frequency coherent event on the field plots (Figure 4). The reflection wavelet appears to be close to minimum phase. The majority of the energy arrives within the first complete cycle. The true two-way reflection time can therefore be chosen at the first identifiable break of the wavelet.

The reflector identified as the bedrock-alluvium interface dominates the recorded data. Energy reflected from anything deeper than the bedrock surface is not observable on field data, since the data were collected primarily within the optimum window for shallow reflections (Hunter et al., 1984) and with relatively severe low-cut filters. Clearly identifiable surface-wave energy is absent from the field plots. The focusing of recorded seismic energy within a narrow target depth window and the lack of surface-wave noise is mainly attributed to the severe low-cut filters and high-frequency geophones.

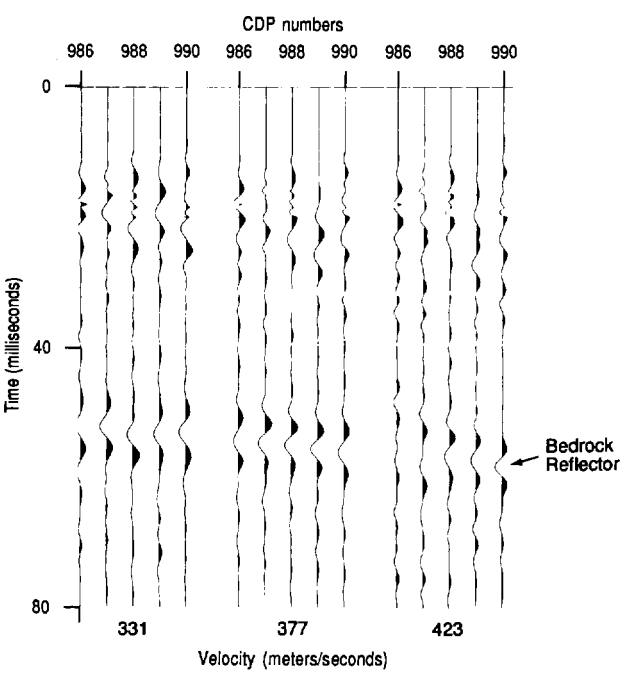

FIG. 3. Stack of 5 CDPs with various velocity values (at bottom of figure) showing drop in frequency and spatial accuracy.

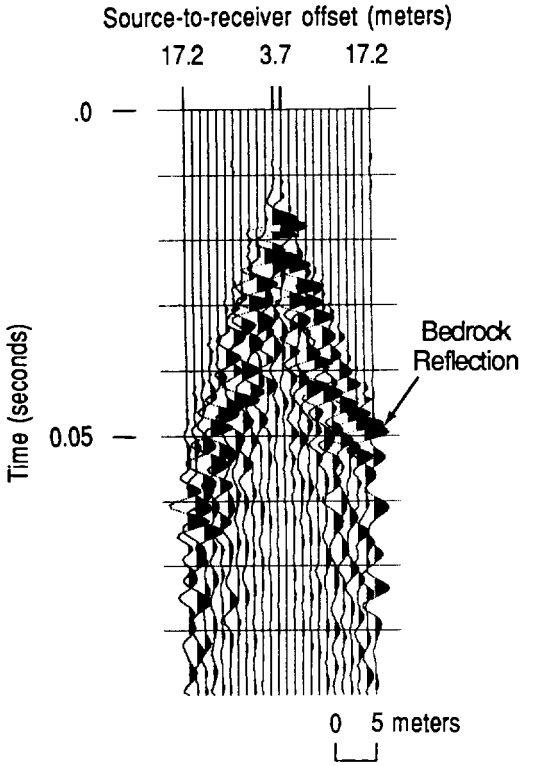

FIG. 4. Field plot identifying bedrock reflector and the air-coupled wave. The air-coupled wave generated by the source is the first arrival.

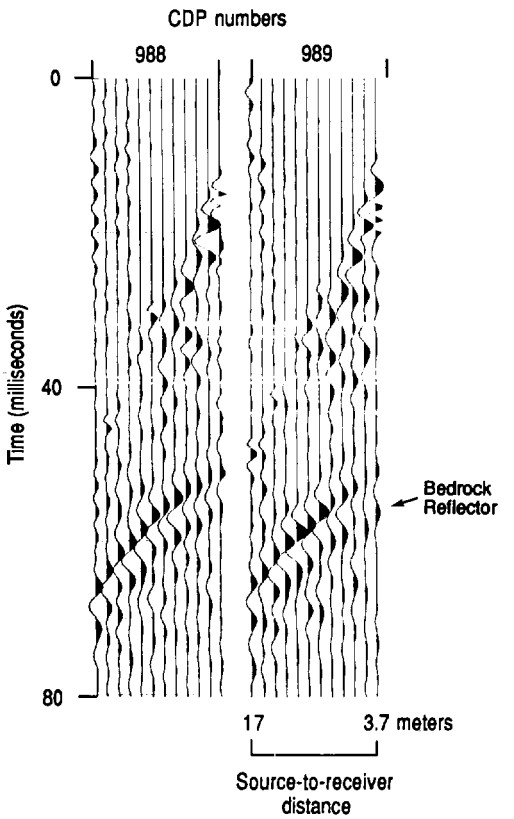

FIG. 5. CDP gathers of 988 and 989. The bedrock reflector can be identified by the characteristic hyperbolic moveout and trace-to-trace coherency. The bedrock reflector has a zero-offset intercept time at these CDPs of about 45 ms.

The bedrock reflector can be identified clearly on the CDP gathers (Figures 5 and 6). Due to the continuous and smooth nature of the reflection on the gathers, a unique NMO velocity can be calculated and applied with a high degree of confidence. From Figures 3 and 6, it is clear that a lack of velocity control could easily decrease the dominant frequency and bandwidth of the final stacked section. With the application of an incorrect NMO velocity, the calculated bedrock depth could be erroneous.

Line 1 traversed the east side of the pond, intersecting line 2, line 3, and the test boring well MW-7 (Figure 7). Data quality is quite good with a discernible bedrock reflection prominent across the entire line. After removal of the refracted arrival by muting, the lone coherent event on the CDP stack is the bedrock reflector. The test-well data confirmed this wavelet as the reflection from the bedrock surface.

The major structural low interpreted on the seismic data of the northernmost line (line 2) at CDP location 940 was previously interpreted from well data only to be present between CDP locations 1000 and 1100 (Figure 8). The secondary bedrock valleys interpreted on the seismic data at CDP 850 were not interpreted on the well data alone (Figure 1). The bedrock surface here, as with line 1, is dominantly the result of erosion. However, this line has sufficient bed offset at CDP 1015 to possibly interpret a bedrock fault. Due to the very localized nature of this offset (not present on line

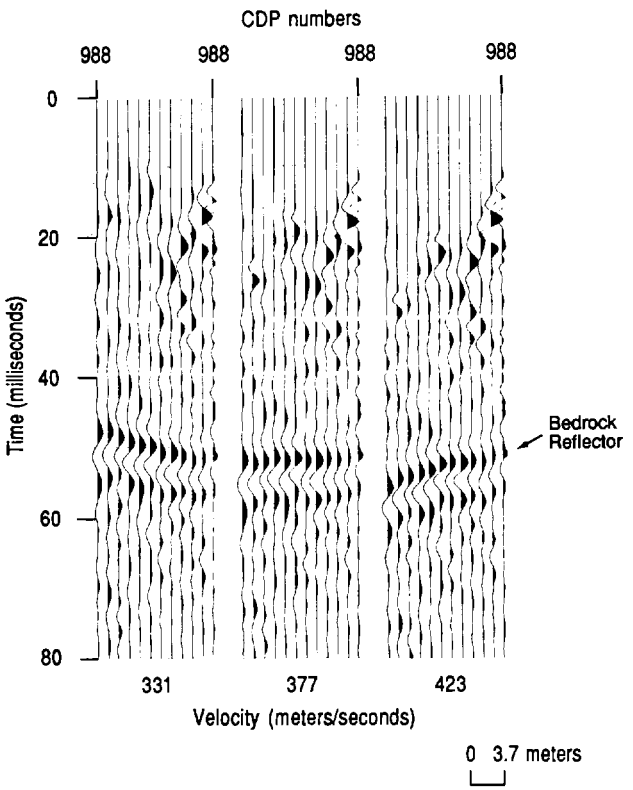

FIG. 6. Velocity analysis of CDP gather 988. CDP 988 has been moved out at three different velocities to show the precision necessary during the velocity analysis stage of the processing flow.

3), no fault is interpreted. The offset is instead assumed to be the result of a subsurface sampling problem that might be resolvable with migration of the data (an option not easily available to us) or of a local dissolution collapse within the red beds.

There are several locations on the stacked sections where faults could be interpreted, such as near CDP 445 on line 1, CDP 870 on line 2, and CDP 1805 on line 3. These tend to be in areas of steep dip of the bedrock-alluvial interface. There are at least three possible explanations for these losses of coherency of the bedrock reflection. First, most of them occur where changes in the velocity model are present. As shown on Figure 3, a slightly incorrect velocity can cause decreased frequency and vertical misplacement of the reflector. Second, as shown by Pullan and Hunter (1985), drastic phase changes in the *P*-wave reflection occur for wide-angle reflections from shallow bedrock. Since the bedrock depth varies by more than a factor of two along these lines, some of the reflections are wide-angle and may exhibit drastic changes in phase at the longer source-receiver offsets. It is possible that these wide-angle reflections locally stack in an incoherent fashion that looks like faults. Another possibility is that there is some distortion of the reflector shape that could be at least partially corrected by migration of the data. It is also possible that combinations of two or more of these effects could occur.

Line 3 represents the southernmost of the two northern lines and continues around the corner of the pond to become the north-south line on the western boundary of the pond (Figure 9). The bedrock topography on line 3 grossly mimics the ground-surface topography. The thickness of alluvium varies from about 6 m at CDP 1800 to 12 m at CDP 2100. Here, as with line 2, the tie to line 1 allows the lone reflecting event to be correlated to the test well data and confidently identified. A bedrock valley is interpreted on the seismic data of line 3 to intersect CDP 1612 on the west and 2016 on the north and to increase in depth to the north. Delineation of this feature was the primary goal of this reflection survey.

The two bedrock contour maps, one derived from drill data (Figure 1) and the other from drill data and seismic data combined (Figure 10), show the interpreted bedrock surface trends of the area at two different resolutions. The potential for misinterpretation of the drill data is evident by the bedrock valley prominent on the seismic-drill contour map (Figure 10) which is missing from the drill contour map (Figure 1). The subsurface sampling interval is 0.6 m for the seismic profile, whereas the drill-data subsurface spacing is roughly 100 m.

The increased subsurface resolution obtained by incorporating seismic-reflection data with the drill data allows accurate placement of a minimum number of wells to monitor fluid levels and water quality. The bedrock valley most likely to channel subsurface alluvial fluids from the pond is located at CDP 939 on line 2 and CDP 2016 on line 3 (accuracy 1 m). A second potential channel for subsurface flow along the bedrock-alluvial interface is at CDP 835 on line 2 and CDP 1864 on line 3. If well placement were determined from drill data alone, the accuracy would be no better than 40 m.

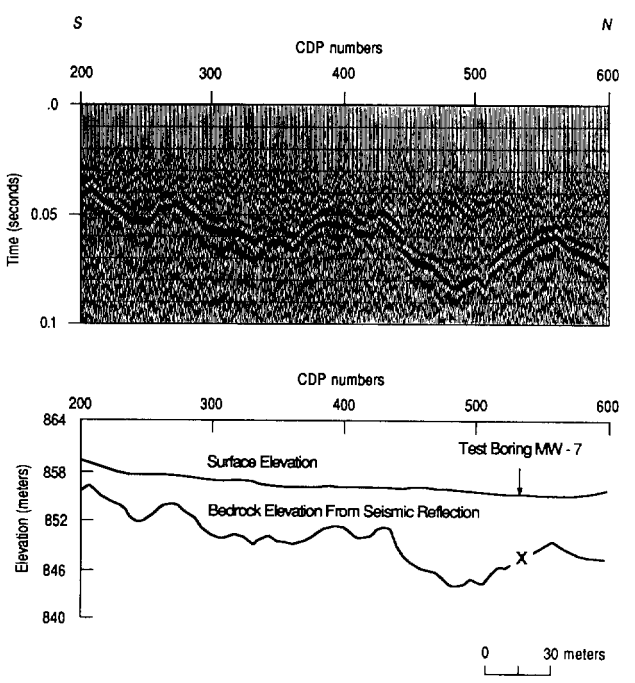

FIG. 7. The 12-fold CDP seismic reflection section of line 1 is at the top of the figure. Bedrock elevation is tied to observed depth of red beds in test boring MW-7 (denoted by x). Line 1 intersects line 2 at CDP 600 and line 3 at CDP 500. Lower half of this figure is elevation cross-section of topography and bedrock surface. Seismic data are static corrected to an 860 m elevation.

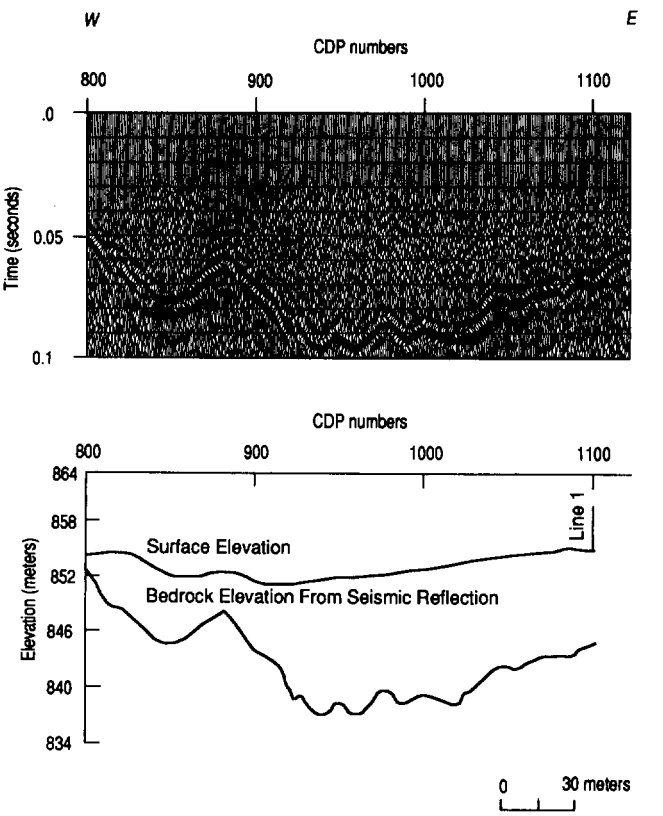

FIG. 8. The 12-fold CDP seismic reflection section of line 2 is at the top of the figure. Lower half of figure is elevation cross-section of topography and bedrock surface. Seismic data are static corrected to 860 m elevation.

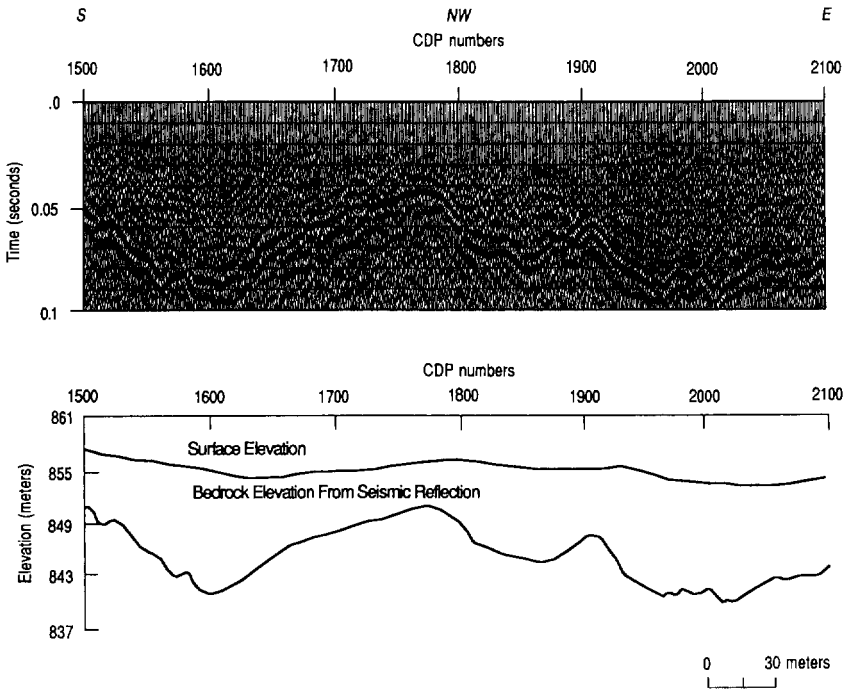

FIG. 9. The 12-fold CDP seismic reflection section of line 3 is at the top of the figure. This line has a nearly right-angle bend in it (compensated for during CDP processing) near CDP 1830 at the highest elevation along the line. Lower half of figure is elevation cross-section of topography and bedrock surface. Seismic data are static corrected to 860 m elevation.

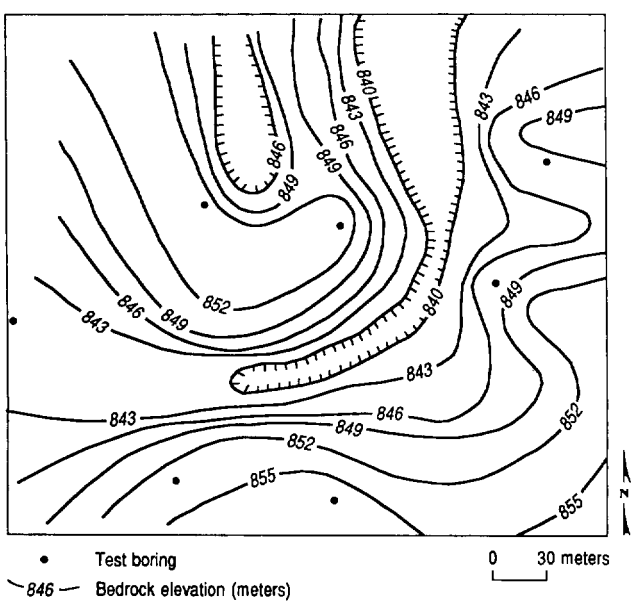

FIG. 10. Bedrock surface topography defined by the three seismic profiles and the borehole information.

CONCLUSIONS

Shallow reflections recorded from the bedrock surface at this Hutchinson County, Texas, site possessed sufficient resolution to identify confidently the major paleodrainage and bedrock lows near an evaporation pond. The dominant recorded frequency of the data was about 170 Hz. The seismic data improved the overall accuracy and precision of the bedrock-structure map by more than an order of magnitude. CDP-by-CDP velocity analysis was necessary to correct properly for the NMO alignment of the bedrock reflector. Without the detailed lateral-velocity analysis, extreme velocity variations over short segments of the line could have resulted in decreased frequency and coherency of the stacked data and erroneous calculations of depth to bedrock. The bedrock reflector varies in two-way traveltime between about 15 ms and 70 ms, which equates to a bedrock depth from about 4 m to 14 m. This much depth fluctuation and velocity variability in the near-surface material could cause serious statics problems for deeper reflection surveys.

The undulation of the seismically defined bedrock surface (Figure 7), as shown on the bedrock-contour map (Figure 10), is indicative of paleodrainage patterns and was not expected to be so dramatically different from present-day topography. The combined seismic-drill data bedrock contour map significantly changed the interpreted structural contours of the bedrock surface derived from the drill data only. The seismic and drill data combined allow for well placement into bedrock lows with accuracy of about 1 m. The critical well locations are at CDPs 939, 835, 1612, 1864,

1968, and 2016. The optimum location for a single monitor well is at CDP 2016 on line 3.

ACKNOWLEDGMENTS

We appreciate the release of this work for publication by Phillips Petroleum Company and Great Plains Geophysical. We would also like to thank Esther Price for her work in manuscript preparation, Marla Adkins-Heljeson for her editorial suggestions, and Pat Acker for the quality graphics work.

REFERENCES

Birkelo, B. A., Steeples, D. W., Miller, R. D., and Sophocleous, M. S., 1987, Seismic-reflection study of a shallow aquifer during a pumping test: Ground Water, **25**, 703–709.

Branham, K. L., and Steeples, D. W., 1988, Cavity detection using high resolution seismic-reflection methods: Mining Eng., **40**, 115–119.

Doornenbal, J. C., and Helbig, K., 1983, High-resolution reflection seismics on a tidal flat in the Dutch Delta—acquisition, processing, and interpretation: First Break, **1**, no. 5, 9–20.

Hunter, J. A., Burns, R. A., and Good, R. L., 1981, Optimum field techniques for bedrock mapping with the multichannel engineering seismograph (abstract): Geophysics, **46**, 451.

Hunter, J. A., Pullan S. E., Burns, R. A., Gagne, R. M., and Good, R. L., 1984, Shallow seismic-reflection mapping of the overburden-bedrock interface with the engineering seismograph—Some simple techniques: Geophysics, **49**, 1381–1385.

Knapp, R. W., and Steeples, D. W., 1986, High-resolution common-depth-point seismic-reflection profiling: Field acquisition parameter design: Geophysics, **51**, 283–294.

Meidav, T., 1969, Hammer reflection seismics in engineering geophysics: Geophysics, **34**, 383–395.

Miller, R. D., Pullan, S. E., Waldner, J. S., and Haeni, F. P., 1986, Field comparison of shallow seismic sources: Geophysics, **51**, 1067–1092.

Miller, R. D., and Steeples, D. W., 1986, Shallow structure from a seismic-reflection profile across the Borah Peak, Idaho, fault scarp: Geophys. Res. Lett., **13**, 953–956.

Myers, P. B., Miller, R. D., and Steeples, D. W., 1987, Shallow seismic-reflection profile of the Meers fault, Comanche County, Oklahoma: Geophys. Res. Lett., **15**, 749–752.

Pakiser, L., and Warrick, R., 1956, A preliminary evaluation of the shallow reflection seismograph: Geophysics, **21**, 388–405.

Pullan, S. E., and Hunter, J. A., 1985, Seismic model studies of the overburden-bedrock reflection: Geophysics, **50**, 1684–1688.

Pullan, S. E., and MacAulay, H. A., 1987, An in-hole shotgun source for engineering seismic surveys: Geophysics, **52**, 985–996.

Schepers, R., 1975, A seismic-reflection method for solving engineering problems: J. Geophys., **41**, 367–384.

Steeples, D. W., and Knapp, R. W., 1982, Reflections from 25 feet or less: 52nd Ann. Internat. Mtg., Soc. Expl. Geophys., Expanded Abstracts, 469–471.

Steeples, D. W., and Miller, R. D., 1986, Some shallow seismic-reflection pitfalls: 56th Ann. Internat. Mtg., Soc. Expl. Geophys., Expanded Abstracts, 101–104.

Treadway, J. A., Steeples, D. W., and Miller, R. D., 1988, Shallow seismic study of a fault scarp near Borah Peak, Idaho: J. Geophys. Res., **93**, 6325–6337.

Widess, W. B., 1973, How thin is a thin bed?: Geophysics, **38**, 1176–1180.